Understanding Self-Assembled Amphiphilic Peptide Supramolecular Structures from Primary Structure Helix Propensity

Martina K. Baumann, Marcus Textor, and Erik Reimhult*

Department of Materials Science, Laboratory for Surface Science and Technology (LSST), ETH Zurich, Zurich, Switzerland

Received May 26, 2008

Small amphiphilic peptides are attractive building blocks to design biocompatible supramolecular structures via self-assembly, with applications in, for example, drug delivery, tissue engineering, and nanotemplating. We address the influence of systematical changes in the amino acid sequence of such peptides on the self-assembled macromolecular structures. For cationic-head surfactant-like eight-residue peptides, the apolar tail amino acids were chosen to systematically vary the propensity to form an α-helical secondary structure while conserving the overall hydrophobicity of the sequence. Characterization of the supramolecular structures indicates that for short peptides a β-sheet secondary structure correlates with ribbonlike assemblies while random-coil and α-helical secondary structures correlate with assembly of rods.

Downloaded via UNIVERSIDADE DO PORTO 01100 on December 2, 2025 at 14:38:50 (UTC).
See https://pubs.acs.org/sharingguidelines for options on how to legitimately share published articles.

Molecular self-assembly has become a widely used method for fabrication of biological and biocompatible structures at the nano- and micrometer range.[1,2] By mimicking how nanostructures are assembled and built with high precision in living cells, artificial model peptides and peptide derivatives have been investigated for their potential to form supramolecular structures.[1,3–6] Key obstacles to form defined structures are understanding and controlling the assembly process. A way to address these issues is to design the primary structure of the peptides to promote formation of the desired structures. The assembly preferences of the monomers can be influenced by, for example, encoding hydrophilic and hydrophobic domains, choosing the primary structure to favor β-sheets or α-helices, or adding charged amino acids.[7–11]

Zhang and co-workers demonstrated that short amphiphilic peptides that mimic the properties of surfactants such as lipid molecules in length and architecture can self-assemble in aqueous solutions to form ordered nanostructures as well as 3D matrix scaffolds.[12–15] However, design of the primary and secondary structure to isolate and identify the effect of a single parameter, such as peptide helix propensity, at low monomer concentration where single supramolecular assemblies of such peptides can be reliably studied has to the best of our knowledge not been demonstrated. Such studies promise to lead to general design principles for amphiphilic peptides from which complex assemblies, such as tubes and vesicles for drug delivery or sheets, wires, and ribbons for templating, can be engineered.

We demonstrate in this letter how different branching modes of the side chains of the amino acids in the hydrophobic part of the amphiphiles yield distinct variations in the (predominantly rodlike) supramolecular aggregates. The rationale behind the choice of the amino acid sequences was to vary only one parameter (i.e., helix propensity[16–18]) in the investigated monomers and relate these variations in primary structure directly to secondary and supramolecular structure adopted in the self-assembled aggregates. Since the cell surface is negatively charged, cationic peptides are of special interest for investigating interactions with cell membranes, for example, for drug delivery applications. Therefore, two lysines were chosen to form the hydrophilic headgroup of the amphiphiles. With a pK_a of 9.76, lysine is positively charged at neutral pH. The aliphatic amino acids leucine, isoleucine, and valine, which all show similar hydrophobicity,[19] were chosen to form the tail of the peptide amphiphiles. Leucine is a γ-branched hydrophobic amino acid that shows a substantial propensity to form α-helical conformation, whereas its β-branched isomer, isoleucine, is known to adopt a β-sheet conformation.[20] In addition, the β-branched amino acid valine was investigated, which shows even lower helix propensity than isoleucine.[18] Nevertheless, it has been shown that polymeric sequences of valine can adopt a helical conformation as well.[21] Furthermore, isoleucine has a chiral side chain, whereas valine and leucine have achiral side chains. Thus, the following three peptides were investigated: Ac-Leu_6Lys_2-NH_2

* To whom correspondence should be addressed. E-mail: erik.reimhult@mat.ethz.ch.

(1) Fairman, R.; Akerfeldt, K. S. *Curr. Opin. Struct. Biol.* **2005**, *15*(4), 453–463.
(2) Whitesides, G. M.; Boncheva, M. *Proc. Natl. Acad. Sci. U.S.A.* **2002**, *99*(8), 4769–4774.
(3) Tsai, C. J.; Zheng, J.; Zanuy, D.; Haspel, N.; Wolfson, H.; Aleman, C.; Nussinov, R. *Proteins* **2007**, *68*(1), 1–12.
(4) Gazit, E. *Chem. Soc. Rev.* **2007**, *36*(8), 1263–1269.
(5) Rajagopal, K.; Schneider, J. P. *Curr. Opin. Struct. Biol.* **2004**, *14*(4), 480–486.
(6) Whitesides, G. M. *Nat. Biotechnol.* **2003**, *21*(10), 1161–1165.
(7) Paramonov, S. E.; Jun, H. W.; Hartgerink, J. D. *J. Am. Chem. Soc.* **2006**, *128*(22), 7291–7298.
(8) Ganesh, S.; Prakash, S.; Jayakumar, R. *Biopolymers* **2003**, *70*(3), 346–354.
(9) Zhang, S. G.; Holmes, T.; Lockshin, C.; Rich, A. *Proc. Natl. Acad. Sci. U.S.A.* **1993**, *90*(8), 3334–3338.
(10) Dong, J. J.; Shokes, J. E.; Scott, R. A.; Lynn, D. G. *J. Am. Chem. Soc.* **2006**, *128*(11), 3540–3542.
(11) Bellomo, E. G.; Wyrsta, M. D.; Pakstis, L.; Pochan, D. J.; Deming, T. J. *Nat. Mater.* **2004**, *3*(4), 244–248.
(12) Santoso, S.; Hwang, W.; Hartman, H.; Zhang, S. G. *Nano Lett.* **2002**, *2*(7), 687–691.
(13) Vauthey, S.; Santoso, S.; Gong, H. Y.; Watson, N.; Zhang, S. G. *Proc. Natl. Acad. Sci. U.S.A.* **2002**, *99*(8), 5355–5360.
(14) von Maltzahn, G.; Vauthey, S.; Santoso, S.; Zhang, S. U. *Langmuir* **2003**, *19*(10), 4332–4337.
(15) Zhang, S. G.; Marini, D. M.; Hwang, W.; Santoso, S. *Curr. Opin. Chem. Biol.* **2002**, *6*(6), 865–871.
(16) Aurora, R.; Creamer, T. P.; Srinivasan, R.; Rose, G. D. *J. Biol. Chem.* **1997**, *272*(3), 1413–1416.
(17) Hermans, J.; Anderson, A. G.; Yun, R. H. *Biochemistry* **1992**, *31*(24), 5646–5653.
(18) Pace, C. N.; Scholtz, J. M. *Biophys. J.* **1998**, *75*(1), 422–427.
(19) Kyte, J.; Doolittle, R. F. *J. Mol. Biol.* **1982**, *157*(1), 105–132.
(20) Arfmann, H. A.; Labitzke, R.; Wagner, K. G. *Biopolymers* **1977**, *16*(8), 1815–1826.
(21) Epand, R. F.; Scheraga, H. A. *Biopolymers* **1968**, *6*(11), 1551.

10.1021/la801605b CCC: $40.75 © 2008 American Chemical Society
Published on Web 07/03/2008

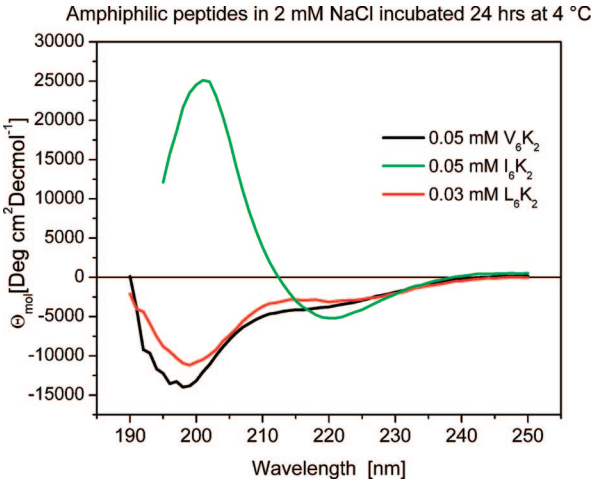

Figure 1. Different secondary structures found for the amphiphilic peptides with different homopolymers of aliphatic amino acids forming the hydrophobic tail. CD spectra were recorded at 20 °C in 2 mM NaCl solution. CD data reveal a β-sheet structure for I6K2 peptides in the assemblies and a random-coil structure for L6K2 and V6K2. All three peptides had stable secondary structures across a wide range of concentrations (0.005 up to 0.1 mM).

(L6K2), Ac-Ile_6Lys_2-NH_2 (I6K2), and Ac-Val_6Lys_2-NH_2 (V6K2). The N-terminus was acetylated to avoid positive charges in the tail region, whereas the C-terminus was amidated.

The high-performance liquid chromatography (HPLC) purified and lyophilized peptides were obtained from Protein and Chemistry Facility, Institute of Biochemistry, University of Lausanne (synthesis protocol, HPLC data, and MS data are available in the Supporting Information). Stock solutions were prepared from the lyophilized peptides (I6K2, 1 mM; L6K2, 0.03 mM; and V6K2, 0.5 mM) in 2 mM NaCl salt solution and diluted to the desired concentration series to study the concentration dependence of the aggregation. Samples were then incubated for 24 h at 4 °C prior to characterization.

The secondary structures of the assembled monomers of all three peptides were constant over the wide range of concentrations that were investigated (0.005 up to 0.1 mM) as determined with circular dichroism spectroscopy (CD), and the typical spectra are shown in Figure 1. For I6K2, a β-sheet secondary structure was found. For both L6K2 and V6K2 peptides, random-coil structures were observed. The shoulder at 222 nm indicative of some α-helical conformation is slightly more pronounced for L6K2 than for V6K2.[22]

For morphological studies of the self-assembled peptide structures, transmission electron microscopy (TEM) with negative staining of aggregates adsorbed onto glow-discharged carbon films was used. Supramolecular structures were observed in different concentration intervals for each peptide and indicated individual critical aggregation concentrations (CAC). The relevant concentration range for investigating the sequence−structure relationship thus varied between the peptides. Determination of the CAC using light scattering was deemed improper due to the polydispersity of the samples. Flat ribbon structures were observed for I6K2 (Figure 2a and b). At 0.01 mM peptide concentration, a helical twist of some ribbons was observed, but since no periodicity could be determined, the twisting does not seem to be an inherent feature of the supramolecular structures. We interpret this as an indication of flexibility of the structures (Figure 2a). At 0.01 mM peptide concentration, structure lengths from

(22) Fasman, G. D. *Circular dichroism and the conformational analysis of biomolecules*; Springer Verlag: Berlin, 1996.

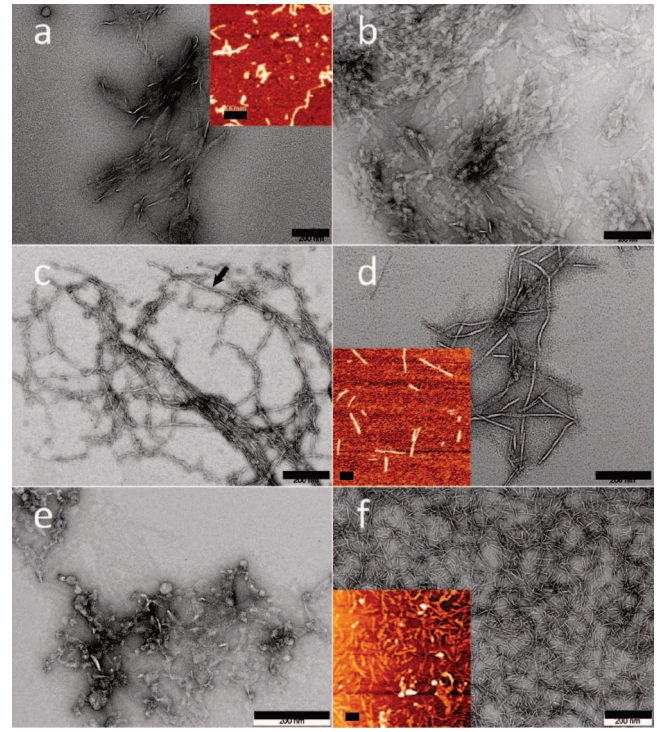

Figure 2. TEM and AFM (insets) micrographs of self-assembled supramolecular peptide structures depict primary sequence dependence of structure formation. (a,b) I6K2. Assembly of flat ribbonlike structures is observed for I6K2 when dissolved in 2 mM NaCl (a, 0.01 mM; b, 0.1 mM). (c,d) V6K2. At lower concentrations (c, 0.05 mM), a superstructure of elongated fibers composed of short fragments is found whereas assembly of rodlike structures is observed for higher concentrations (d, 0.5 mM) when dissolved in 2 mM NaCl. (e,f) L6K2. Assembly of mixed structures (e, 0.005 mM) and formation of rodlike structures at higher concentration (f, 0.03 mM) are found for L6K2 dissolved in 2 mM NaCl. The scale bars in all pictures correspond to 200 nm.

Table 1. Calculated Bulk Parameters for Rodlike Structures[a]

peptide amphiphile	measured width (nm)	measured height (nm)	bulk radius (nm)
V6K2	13	2.2	3.0
L6K2	6	1.3	1.6

[a] Structures detected in AFM and TEM micrographs are thought to be collapsed during adsorption and drying on hydrophilic surfaces before imaging. The rectangular area calculated with rod width and height found with TEM and AFM was assumed to correspond to the circular cross sections of the bulk structures and the corresponding radius calculated.

100 up to 600 nm were found. For higher concentration (0.1 mM), shorter structures and a more narrow length distribution between 80 and 360 nm were found while the ribbon widths increased from 30 nm up to flat sheetlike formations (Figure 2b). Complementary tapping-mode atomic force microscopy (AFM) measurements in air confirmed the structures found with TEM and indicated a structure height of 3.7−4 nm (inset of Figure 2a and Table 1). V6K2 was found to form thin rodlike structures from short fragments (30−100 nm) to elongated rods (up to 400 nm) at 0.05 mM peptide concentration. They aggregate to form fibers in the micrometer range (Figure 2c). Thereby, the rods coalign and some twist around each other (arrow in Figure 2c). For higher concentration (0.5 mM), the formation of compact rods with diameters of approximately 13 nm and lengths of 50−350 nm was observed (Figure 2d). AFM data revealed a structure height of approximately 2.2 nm (Table 1) and confirmed the formation of rodlike structures (inset of Figure 2d). L6K2 showed amorphous aggregates at lower concentrations (Figure 2e) and formation of thin rods of 50−100 nm length and 6 nm

in diameter at 0.03 mM peptide concentration (Figure 2f). AFM data support the formation of rodlike structures with measured heights of 1.3 nm (inset of Figure 2f and Table 1).

Thus, we observed that at lower peptide concentrations (0.05−0.1 mM) in aqueous solution rod- and sheetlike supramolecular structures with different cross sections are formed for each of the investigated peptides. The amino acid sequences adopting predominantly random-coil structures (V6K2 and L6K2) lead to the formation of compact rodlike structures with discrete cross sections for each peptide but varying in rod length. Thereby, L6K2 starts to form compact rod structures at 0.03 mM peptide concentration, whereas for V6K2 compact rods were detected at 0.5 mM peptide concentration. The β-sheet forming peptide I6K2 aggregates to broader sheetlike structures, which show an increasing cross section with increasing peptide concentration.

Since the surfaces used for characterization are hydrophilic, the structures detected with AFM and TEM are considered to be supramolecular structures from solution that collapsed during adsorption and subsequent drying. The great similarity of structures, the clear concentration dependence of the observed structures, and the quick drying in relation to the apparent stability of the structures strongly indicate that the transient concentration change during drying does not significantly affect the aggregate structures. However, the asymmetric dimensions of the dried out assemblies observed on the surface indicate collapse during the drying step (see Schematic 1 in the Supporting Information), which requires reconstruction to estimate the likely 3D structure in bulk solution. The measured structure height of I6K2 agrees to the length of two monomers (each ~2 nm) and indicates bilayer formation stable to drying, whereas the measured structure heights of V6K2 as well as L6K2 correspond to the length of one monomer and are likely to reflect unfolding upon drying, since such an amphiphilic asymmetric structure is not expected to be stable in bulk aqueous solution. Thus, it seems that the β-sheet forming peptide I6K2 results in bilayer ribbon superstructures in bulk solution, while we propose that the random forming V6K2 and L6K2 produce micellar rodlike bulk superstructures. To confirm this, we estimated a bulk radius for the assumed rods by calculating the rectangular area using structure width and height obtained by TEM and AFM and assuming the area would correspond to the cross section of the structure in bulk solution (see Table 1). The calculated bulk radii both seem to correspond to micellar structures (approximately one monomer in length), and L6K2 appears to be more densely packed than V6K2. It is noteworthy that L6K2 shows the most shallow adsorbed structure height. Since it is the peptide monomer with the highest helix propensity and also has the most pronounced α-helical shoulder in the CD measurements, this could indicate a tendency toward a helical secondary structure leading to a shortening of the monomer length. Despite being at different ends of the helix propensity scale used for designing the hydrophobic tail of the amphiphiles, valine and leucine containing sequences generate similar supramolecular structures. Thus, the main differences in macromolecular structures seem to arise from the ability to form β-sheet interactions between the monomers. For V6K2 and L6K2, hydrophobic interactions are the sole driving force for self-assembly, since there is no specific hydrogen bonding among the amphiphile segments, while for I6K2 β-sheet hydrogen bonding plays a role (Figure 1). Furthermore, isoleucine has a chiral side chain, whereas valine and leucine have achiral side chains. Together with hydrogen bond formation, chirality can be a factor to induce a different type of supramolecular packing for I6K2. The observation that V6K2 adopts a random-coil conformation also in the supramolecular aggregates thus agrees better with previous observations of valine polymers adopting α-helical conformation[21] than with predictions based on occurrence frequency in protein domains suggesting β-sheet preference.[18]

In summary, we have demonstrated that primary and secondary structure design is a feasible tool to generate different rod- and sheetlike supramolecular assemblies, including tuning aggregate shape and width, as well as a possible tool for predicting supramolecular structure. In particular, we have shown that for these short amphiphilic diblock peptides coding the hydrophobic tail to form β-sheets induces the formation of sheets, while the absence of β-sheet hydrogen bonding for similar peptides yields micellar rods. We have also demonstrated that monomer concentration can be used to tune average rod length and ribbon/sheet area over a large range.

Acknowledgment. We thank the Swiss National Science Foundation, NCCR Project "Nanoscale Science" for funding this project. The authors acknowledge support from the Electron Microscopy ETH Zürich, EMEZ, and Dr. Salvatore Chessari for discussions.

Supporting Information Available: Preparation protocols for peptide sample solutions, AFM specimens, and TEM specimens, measurement parameters for AFM, TEM, and CD, as well as HPLC and MS data for the peptide samples. This material is available free of charge via the Internet at http://pubs.acs.org.

LA801605B